Evaluation of hydroxyapatite- and zinc-coated Ti-6Al-4V surface for biomedical application using electrochemical process

Rakesh Kumar [1] · R. Thanigaivelan [2] (ORCID) · G. K. Rajanikant [3] · T. Jagadeesha [1] · Jyotirekha Das [3]

Abstract

In this research, the cell viability is tested on the surface-modified implants. Electrochemical setup is used for coating the hydroxyapatite (HA) powder and nano zinc particle $(Zn)_n$ on the Ti-6Al-4 V alloy. The electrolyte is prepared by mixing the HA and $(Zn)_n$ of varying quantity, and the effect of electrochemical parameter on surface coating thickness, surface quality and cell viability was studied. Based on the study, the cell viability is observed to be maximum at HA and $(Zn)_n$ concentration of 6 g/L and 0.8 g/L, respectively. The $(Zn)_n$ concentration in the range of 0.8 to 1.2 g/L and voltage of 12–13 V is suitable for obtaining the controlled coating thickness. During the electrochemical process, the nanopores HA structures with a pore size of 215–786 nm are obtained attributes for better cells attachment on the surface. The cell viability is found high (0.366) at 6 g/L HA and 1.6 g/L of $(Zn)_n$ concentration at 14 V.

Keywords Electrochemical deposition · Hydroxyapatite · $(Zn)_n$ · Skewness · Cell viability · Coating · Surface roughness

Introduction

The demand for metallic biomaterials-based medical devices is increasing day by day, and there is a requirement for the development of biomaterials which owns the identical characteristics to human bones [1]. Metallic materials, such as stainless steel, cobalt-chromium and titanium and its alloys, have been used as orthopaedic implants [2]. Remarkable biocompatibility and favourable mechanical properties of titanium and its alloys have involved huge interest among researchers. Research studies have exposed that Ti-6Al-4 V is the mostly used Ti alloy in an orthopaedic application for knee and hip prosthesis bone screw and plate, because of their excellent characteristics such as high specific strength, superior resistance to corrosion and absolute inert to the bodily fluid [3–5]. Even if Ti and its alloy fulfil most of the needs of implant material, they will be incapable in meeting the needs of osseointegration which provides competent binding to surrounding tissues and bone, because of their inactive surface characteristics, their poor tribological properties like low wear resistance and low surface hardness of material [6]. Now, modifying the surface of titanium-based implant through mechanical, physical, chemical or biochemical treatments becomes mandatory to enhance the biological performances of osseointegrated implants [7]. Previously in an experiment, the pretreated Ti alloys plates were coated using pure HA, and this pretreatment process shows significant effect on mechanical properties and the surface exhibited the highest cell proliferation and lowest bacterial adhesion [8]. The ability of HA coating helps to integrate implant to the bone and support new bone generation and surface protection against body fluid. The porous nature of HA ceramic

✉ R. Thanigaivelan
tvelan10@gmail.com

Rakesh Kumar
rakeshguptaa0007@gmail.com

G. K. Rajanikant
rajanikant@nitc.ac.in

T. Jagadeesha
jagdishsg@nitc.ac.in

Jyotirekha Das
jyotirekha.das5@gmail.com

1 Department of Mechanical Engineering, National Institute of Technology, Calicut, Kerala 673601, India

2 Department of Mechanical Engineering, Muthayammal Engineering College (Autonomous), Rasipuram 637408, India

3 School of Biotechnology, National Institute of Technology, Calicut, Kerala 673601, India

coating provides high surface area leading to excellent osteoconductivity, resorbability providing fast bone in growth and sufficient bioactivity for its partial resorption leading to successful replacement of natural bone cells. Moreover, it can create strong chemical bonds with bones [9, 10]. The electrophoretic deposition method is used to coat nanoparticles HA onto Ti6Al4V alloy and studied the effect of voltage and coating time on deposition rate, coating thickness and surface area coverage. The best HA coating was obtained at 5 V for 5 min, coating thickness is 79.13 μm, and surface coverage is 97.89% [11]. Further zinc (Zn) is well-known for its inherent antimicrobial property and thus has been applied extensively as antibacterial materials, including ZnO films, Zn-incorporated coatings [12]. Given that, various surface modification techniques, such as chemical vapour deposition, plasma electrolytic oxidation (PEO), physical vapour deposition and anodizing, had been used [13, 14]. Plasma spraying is the most widely used technique for coating, but it results in decomposition of HA due to the high-temperature environment, and it is not suitable for complex structures. In an electrophoretic deposition, high voltage was applied to the metal surface to attract the dispersed particles which lead to anodic polarization of metal substrate. This might increase the corrosion risk of metal and suppress the adhesion of HA particles [15–17]. Nano-biphasic bio-ceramic coating (NBBC) on 316 L stainless steel is performed and characterized using XRD, FTIR, FESEM with EDAX and AFM. The study confirms that NBBC coating enhances the corrosion resistance, mechanical strength and cell attachment and proliferation making suitable for orthopaedic implants [18]. Among all modification methods, electrochemical deposition is found to be advantages due to its simplicity, low cost, generation of inert surface and excellent control of deposition. Qiu et al. [19] prepared and characterized the HA/titania composite coating on NiTi alloy by electrochemical deposition. Yan et al. [20] have prepared the HA-/gelatin-functionalized graphene oxide coating using electrodeposition method. Hence, researchers have considered electrochemical deposition for HA and other materials. In this research, the HA and $(Zn)_n$ are used to coat the specimen. Moreover, zinc-modified implant surface with HA improves the osteoblastic function and bone integration with implant surfaces. The advantage of the Zn merged HA decreases the crystallinity of HA and enhances production and differentiation of osteoblasts [21]. In this research, the effect of varying quantity of HA with $(Zn)_n$ mixed electrolyte on surface roughness, cell viability and coating thickness was studied. Moreover, this surface modification process is simple and economical compared with other processes. The aim of the present study was also to investigate the effect of surface geometrical features on cell viability.

Methodology

Sample preparation

Ti-6Al-4 V (grade 5) was chosen as implant material in the present study. The chemical composition of implant material was verified through energy dispersive X-ray spectrometry (EDS) made of EVO MA18. The samples with dimension $30 \times 30 \times 0.5$ mm were cut from a sheet by using a power shearing machine, and all the measurements are taken at the centre region of the specimen. Firstly, implant material was ground to average surface roughness (Sa) of 389.27 nm. Pure copper was used as tool electrode during the electrochemical process. An aqueous solution of citric acid (0.208 mol/L) was used as an electrolyte. The citric acid is mixed with distilled water and mixed thoroughly using stirrer. Pure HA powder (99.5 wt.%) with average particle size 20.40 nm and $(Zn)_n$ (Zn, purity 99.9 wt.%, 30–50 nm metal basis) was added to the electrolyte to obtain a range of concentrations. HA with a range of concentrations (0, 6, 10, 14 g/L), $(Zn)_n$ with a range of concentrations (0.4, 0.8, 1.2, 1.6 g/L) and anodic voltage range of 11 to 14 V were used. The inter-electrode gap of 1 mm is maintained between anode and cathode. Other electrochemical parameters are kept constant for all experiments. The machining condition was selected based on the previous studies, and pulsed power supply duty ratio is kept constant at 80% throughout the experiments. The surface coating was done for 30 min, and then the implants were kept for 10 min in the open air, cleaned using an ultrasonic cleaner with acetone and dried by using a hairdryer. The surface roughness was measured using 3D optical profilometer Alicona Infinite Focus G5 using a cutoff wavelength of 324.23 μm. To minimize the measurement error, measurement was repeated four times, and the average value was taken. The microstructures were observed by FE-SEM made of Hitachi SU6600. The composition of HA-$(Zn)_n$-coated implant was verified, and the distribution of elements on the coated surface was checked by energy dispersive x-ray spectroscopy (EDS) made of EVO MA18. Surface coating thickness was measured by using a coating thickness gauge (Surfix ® Pro S, PHYNIX Germany). The schematic of the electrochemical setup is shown in Fig. 1. The process parameters and levels used for surface coating are presented in Table 1.

Cell culture and MTT assays

MG-63 cell culture

MG-63 cells (ATCC® CRL-1427™) were procured from National Centre for Cell Science, Pune, India, cultured in Dulbecco's modified Eagle's medium (DMEM)/F12 (Thermo Fisher Scientific, MA, USA) supplemented with 10% fetal bovine serum (FBS) and 1% penicillin-streptomycin (Thermo Fisher Scientific, MA, USA) at

Table 1 Surface coating conditions at constant electrolyte concentration and IEG

Implant sample Designation.	HA(g/L)	$(Zn)_n$ (g/L)	Voltage	Surface roughness (Sa, μm)	Cell viability (OD)	Coating thickness (μm)
a	–	1.6	14	0.368	0.242	0.875
b	6	1.6	14	0.734	0.366	5.20
c	10	1.6	14	0.348	0.212	6.80
d	14	1.6	14	2.941	0.146	14.76
e	14	0.4	14	0.543	0.148	4.30
f	14	0.8	14	0.558	0.235	5.25
g	14	1.2	14	0.613	0.222	10.75
h	14	1.6	14	2.941	0.146	14.76
i	14	1.6	11	0.538	0.166	8.47
j	14	1.6	12	0.692	0.189	9.46
k	14	1.6	13	1.189	0.307	12.65
l	14	1.6	14	2.941	0.146	14.76

37 °C. The cells are incubated in a humidified atmosphere containing 5% CO_2 and 95% air and allowed to grow up to 70% confluency and trypsinized using 0.25% trypsin/EDTA (Thermo Fisher Scientific, MA, USA). The cells were then seeded on presterilized implants at a density of 5×10^5 cells/implant. These implants were kept in the 24-well plates (Thermo Fisher Scientific, MA, USA) to carry out further experiments. The MTT assay tests are repeated for 2 times, and the average values of cell viability, surface roughness and coating thickness are provided in Table 1.

Cell viability assay

To perform the 3-(4,5-dimethylthiazol-2-yl)-2,5-diphenyltet-razolium bromide (MTT) assay, the cells were cultured in the culture plate as primary control and on the various implant materials at a density of 5×10^5 cells/well/implant for 24 h. On the 24th hour, the cells were harvested for the MTT assay, and the media was removed, washed with PBS solution for three times. Following this, the fresh media containing the MTT reagent (0.5 mg/ml) (Thermo Fisher Scientific, MA, USA) has been added to the wells. The plates were incubated at 37 °C for 3–4 h, and sodium dodecyl sulphate (10% SDS in 0.01 M HCl) was added to the solution to dissolve the formazan crystals formed by the MTT reagent.

The cells were further incubated overnight at 37 °C for complete solubilization of the formazan crystals. Following this, the medium was transferred to another 24-well plate (Thermo Fisher Scientific, MA, USA), and the absorbance was recorded at 570 nm using a multimode microplate reader

Fig. 1 Schematic diagram of the experimental setup
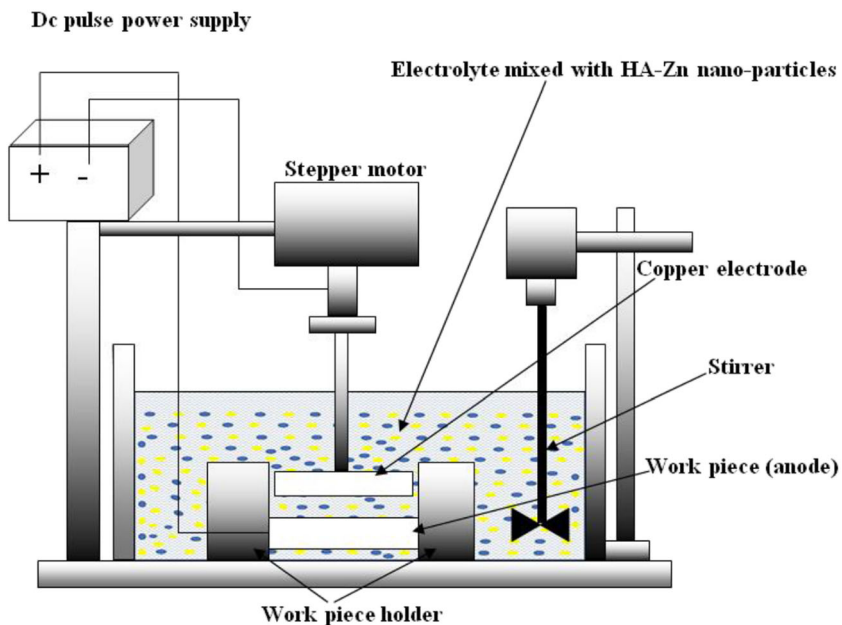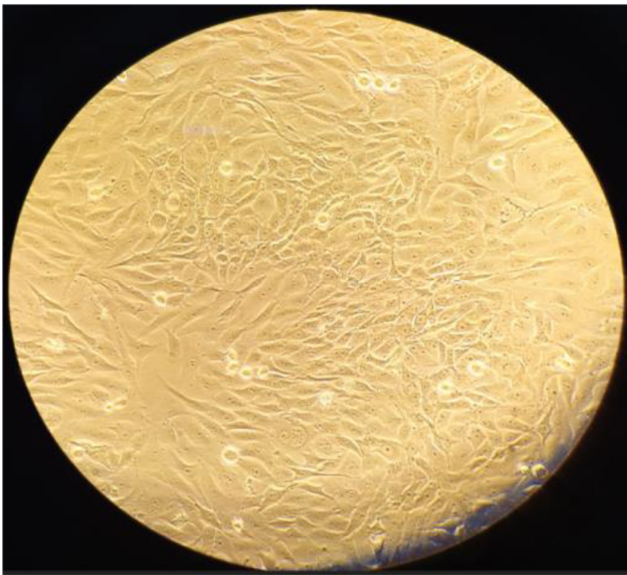
Fig. 2 Microscopic image of control sample

(TECAN, Infinite200 pro, Switzerland). Figure 2 shows the microscopic image of control samples.

Results

Effect of HA concentration

Figure 3 shows the effect of change in HA concentration on surface roughness, cell viability and coating thickness. It is observed that the increase in HA concentration increases the surface roughness less linearly and again decreases then increases drastically. At higher concentration of HA, the surface roughness increases drastically. It is because at higher HA
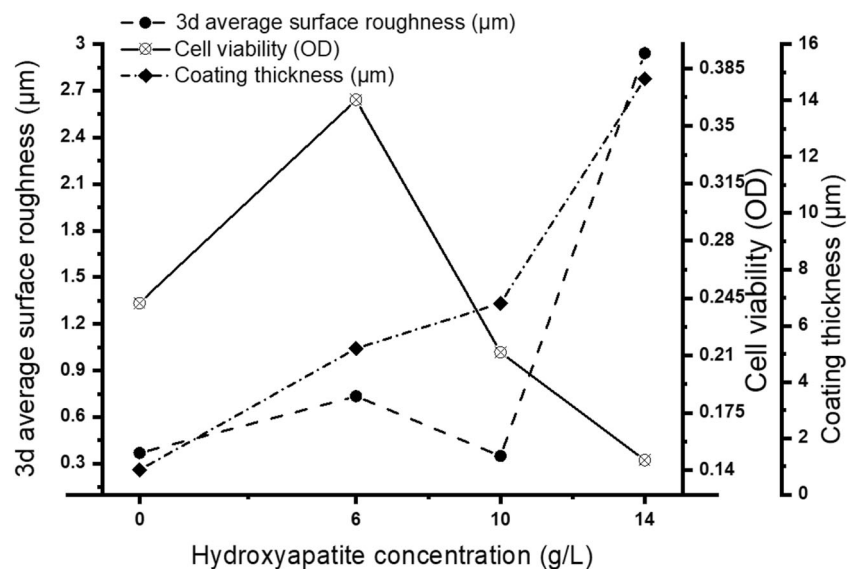
concentration, the availability of HA in the electrolyte is more. Rather than the HA concentration, the electrical parameters such as voltage and duty cycle are maintained at 14 V and 80% duty cycle, respectively, which aid the rapid deposition of the HA on the implant. At higher voltage and duty cycle, the generation and breakdown of hydrogen bubbles in the cathode flash the HA and spread the deposition across the implant. The breakdown of numerous bubbles deposits the HA with micro-/nano-sized craters and pits, leading to higher surface roughness. The coating thickness increases less linearly from 6 to 10 g/L of HA concentration and reaches its highest value for 14 g/L of HA concentration. The surface roughness is found to be 0.734 μm which facilitates the better cell viability, proliferation to the surfaces. A cluster of micropores in nm size, which will assist cell attachment and its easy culture on the surface. The nanoporous HA structures increase the surface area by 20 to 30%; now, this excess area facilitates cells to adhere to the titanium plate convincingly. Thus, electrochemical process parameters with varying concentration of HA contribute to the generation of surface roughness in the range of 0.368 to 2.941 μm and cell viability in the range of 0.146 to 0.366 OD.

Figure 4 a–d show the surface morphology of implant with and without HA-$(Zn)_n$ coating at HA concentration of 0 g/L, 6 g/L, 10 g/L and 14 g/L for same working conditions. The cell viability is observed to be maximum at HA concentration of 6 g/L, and surface roughness is found to be 0.734 μm. A cluster of micropores of size 379 to 786 nm was observed at 6 g/L concentration in Fig. 4b. At HA concentration of 10 g/l, the more dense and uniform coated surface was observed which leads to lower surface roughness (Fig. 4c). At higher concentration of HA (i.e. 14 g/L), the distribution of multiple shallow micro-craters and micro-cracks was observed (Fig. 4d), which leads to higher surface roughness.

Fig. 3 Effect of change in HAP concentration on surface roughness, cell viability and coating thickness

Fig. 4 SEM images of (**a**) anodic coating without HA (**b**) coating with 6 g/L concentration, (**c**) coating with 10 g/L concentration and (**d**) coating with 14 g/L concentration
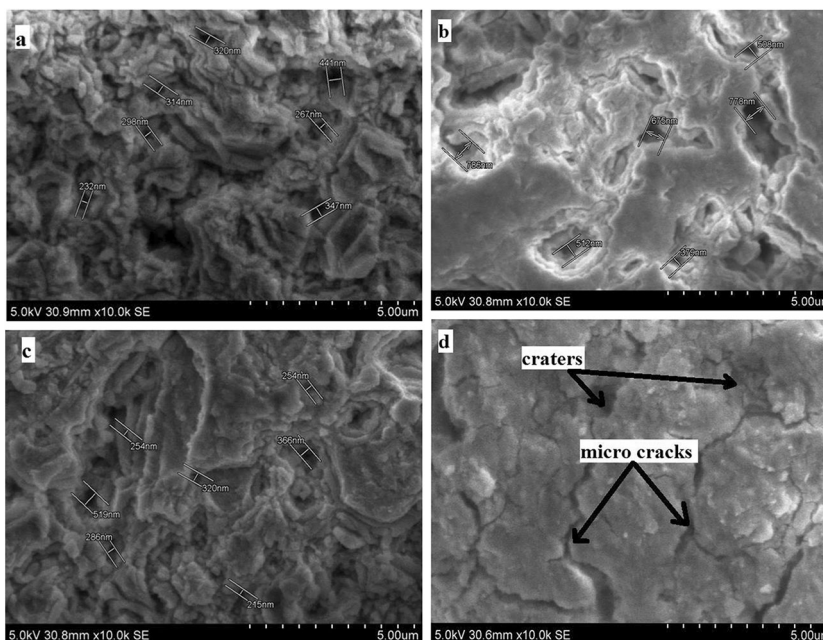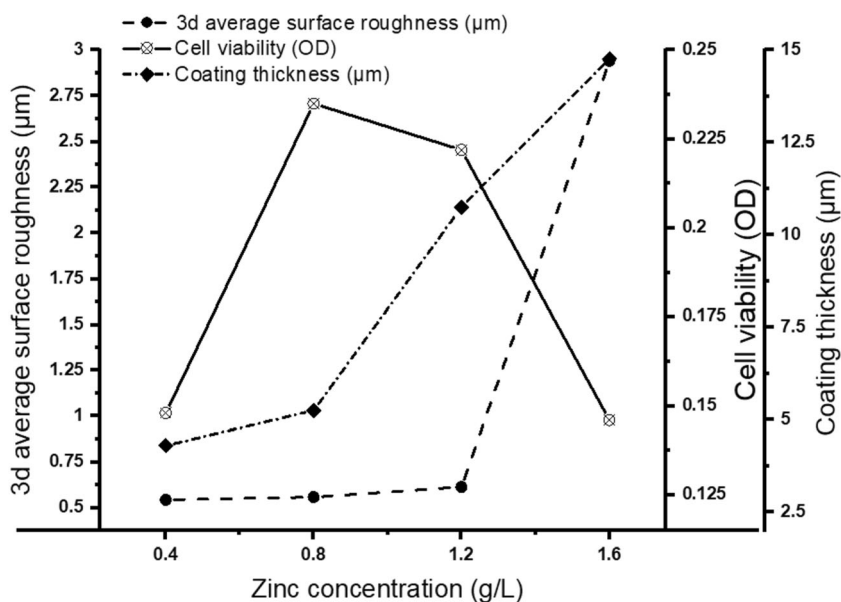

Effect of (Zn)$_n$ concentration

From Fig. 5, it can be observed that there is an abrupt increment in surface roughness after 1.2 g/L concentration of (Zn)$_n$. A significant decrease in cell viability was found with excess zinc concentration. Cell viability was found to be maximum at (Zn)$_n$ concentration of 0.8 g/L. A very fine pores size in the range of 196 to 611 nm was observed in Fig. 6a. Figure 6 b shows the narrow and wide micro-cracks. Figure 6 c shows the size of the minimum nanopore of 303 nm and maximum size of 844 nm. Figure 6 d shows the coating with lesser cracks. The coating thickness is also found to increase linearly with (Zn)$_n$ concentration. The (Zn)$_n$ concentration in the range of 0.8 to 1.2 g/l is suitable for obtaining the controlled coating thickness. The minimum coating thickness achieved on the implant was 4.30 μm.

Addition of (Zn)$_n$ plays a vital role in the preservation of bone mass and promotes alkaline phosphatase activity [21]. In this study, by the way of adding (Zn)$_n$ increases the localization effect by increasing the current density which further enhances the deposition rate of HA which in turn increases micropores size. This kind of microporous surfaces provide huge exposure which facilitates medium for cell proliferation, and the cell gets easily attached to it. Sometimes surface roughness alone cannot determine the amount of cell viability. There is a need to address some other surface characteristics

Fig. 5 Effect of (Zn)$_n$ concentration on surface roughness, cell viability and coating thickness
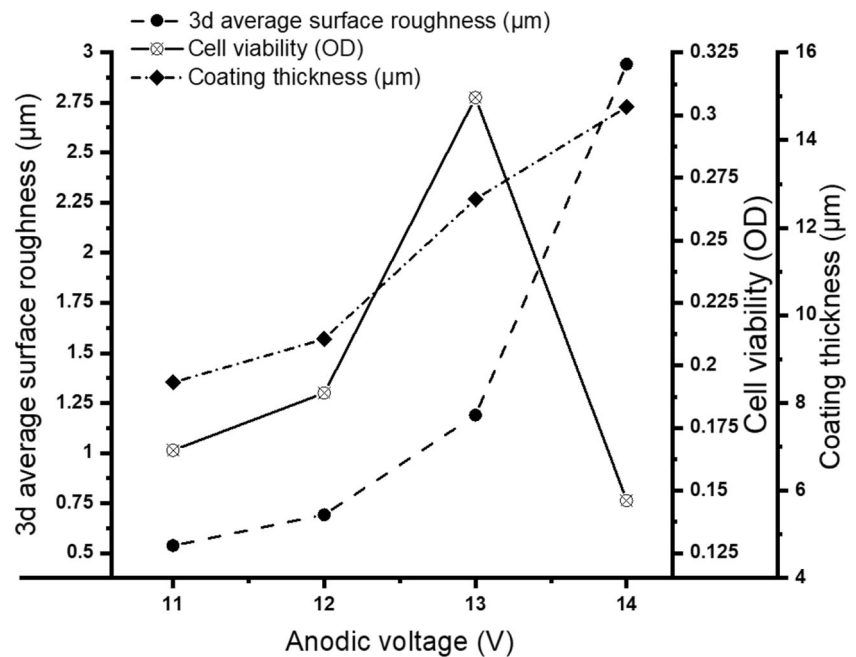
Fig. 6 SEM surface morphology of implant at (**a**) $(Zn)_n$ concentration of 0.4 g/L, (**b**) $(Zn)_n$ concentration of 0.8 g/L, (**c**) $(Zn)_n$ concentration of 1.2 g/L and (**d**) $(Zn)_n$ concentration of 1.6 g/L
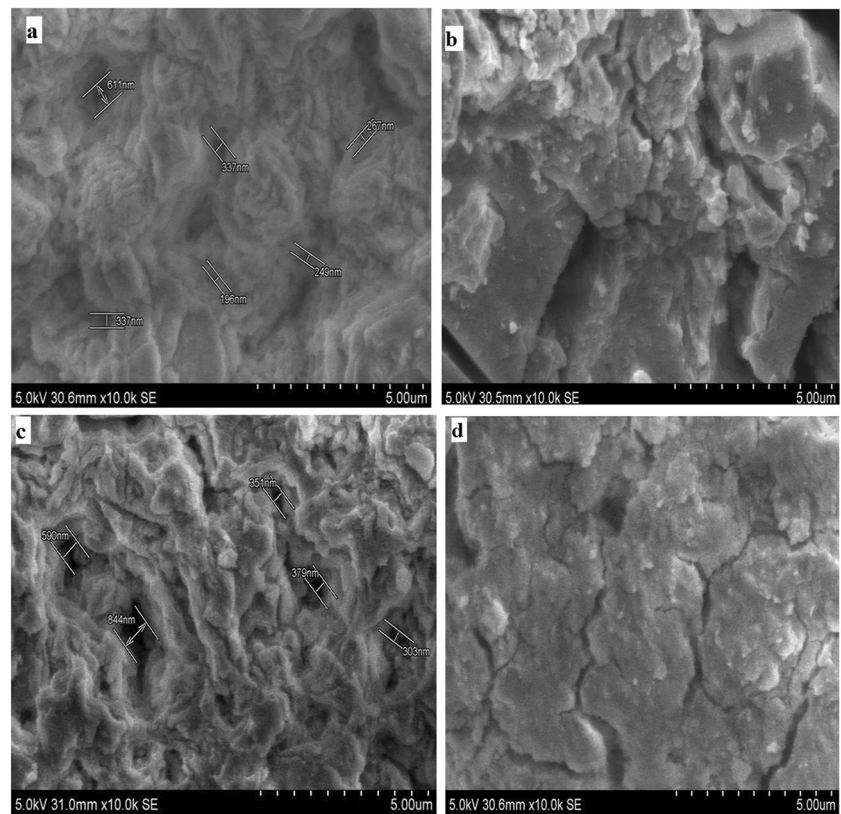
like skewness; from this experiment, it is found that the negative skewness indicates that the broader peaks provide larger surface exposure for cell growth to take place [22]. SEM images depict that with an increase in the concentration of zinc, the size of pores increases contributing to negative skewness and enhancement of surface roughness.

Effect of anodic voltage

Figure 7 shows the effect of anodic voltage on surface roughness, cell viability and coating thickness. As the voltage increases, the coating thickness and surface roughness increase less linearly. Further increase in voltage the coating thickness
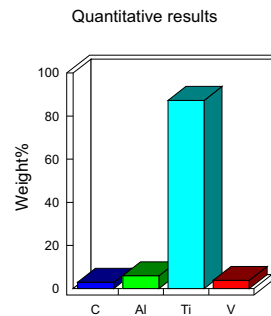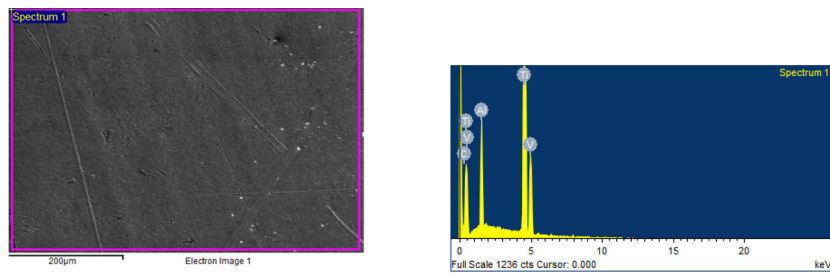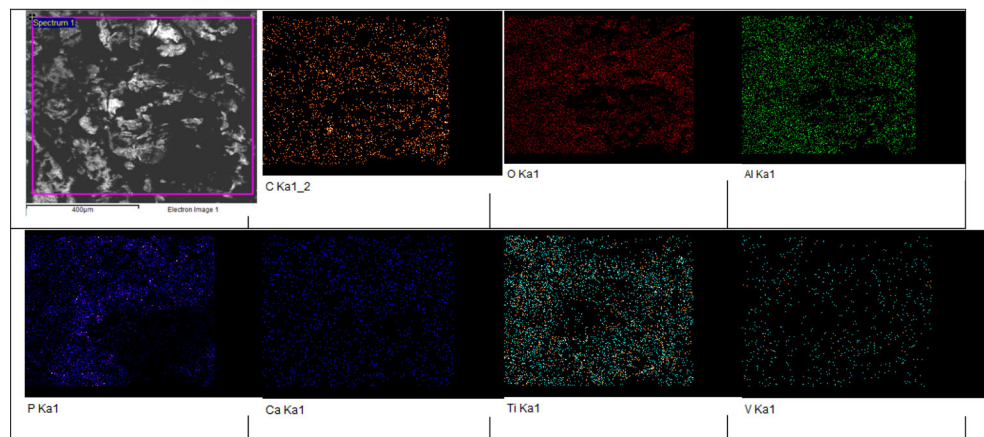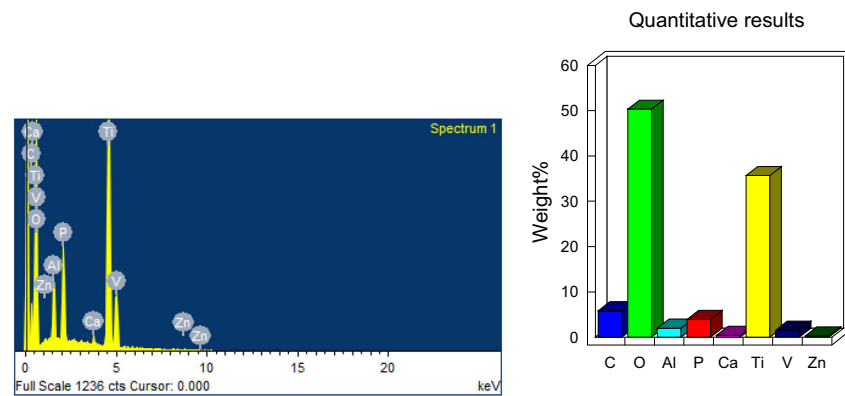
Fig. 7 Effect of anodic voltage on surface roughness, cell viability and surface coating thickness

Fig. 8 (**a**) SEM image and EDS elemental mapping of implant surface before coating. (**b**) EDS elemental mapping of HA-(Zn)$_n$ coated surface
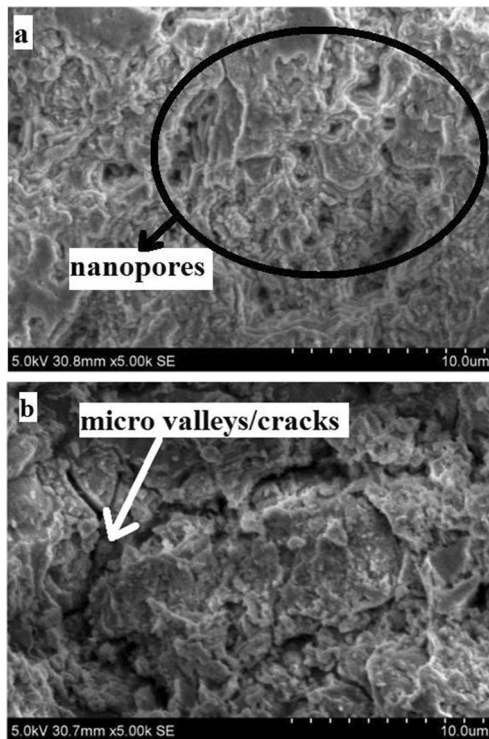

a   SEM image and EDS elemental mapping of implant surface before coating

b   EDS elemental mapping of HA-(Zn)n coated surface

increases linearly. Hence, it is evident that the voltage range of 12–13 V is suitable for obtaining the controlled coating thickness. The anodic voltage has a significant impact on the surface modification of the implants. Researchers have

Fig. 9 SEM images of the coated implant with (**a**) 10 g/L HA and 1.6 g/L of (Zn)$_n$ and (**b**) 14 g/L HA and 1.6 g/L of (Zn)$_n$

Table 2 Surface characteristics as a function of surface coating conditions

Implant sample designation	Surface coating condition	Ssk	Sku
a	HA 0 g/L	−0.401	4.405
b	HA 6 g/L	−0.856	4.599
c	HA 10 g/L	−0.271	5.587
d	HA 14 g/L	−0.560	6.544
e	Zn 0.4 g/L	2.059	8.686
f	Zn 0.8 g/L	0.269	7.559
g	Zn 1.2 g/L	1.524	5.148
h	Zn 1.6 g/L	−0.560	6.544
i	Volt 11v	1.308	10.891
j	Volt 12v	0.985	12.581
k	Volt 13v	−0.639	4.703
l	Volt 14v	−0.560	6.544

reported that the increase in electrode potential in electrochemical reaction contributes to growth of oxide layers on the titanium surfaces [13, 23]. Hence, the rate of reaction is affected by anodic voltage; higher anodic voltage will make the oxide film larger. Increasing current density increases both the ion exchange rate in the barrier and increases the deposition rate of the porous HA. Presence of C, O, Al, P, Ca, Ti and Zn over the coated surface indicates that HA-Zn has been coated successfully. The presence of oxygen is evident for the formation of the strong oxide layer over the surface; the porous surface morphology of obtained layers of TiO$_2$ is also

beneficial for bio-interactions between bone cells and proteins [24]. After anodic oxidation, the percentage weight of oxygen increased considerably, whereas that of titanium decreased from 90 to 39%.

Figure 8 a shows SEM images and EDS mapping of implant surface before coating. By EDS mapping aids, it shows the %weight composition of the material. The presences of oxides are noticed in the Fig. 8b after electrochemical deposition of HA-(Zn)$_n$ powder.

Figure 9 a and b show the SEM images of the coated implants which clearly shows that the HA-(Zn)$_n$ concentration has a significant effect on the functional properties of the coated surface. The presences of nanopores and micro valleys are noticed on the SEM pictures. The application of electrochemical deposition provides a dense and uniform HA-(Zn)$_n$ coating with a cluster of nanopores. The deep micro-craters/micro-cracks on the implant for a higher concentration of HA are leading to higher surface roughness.

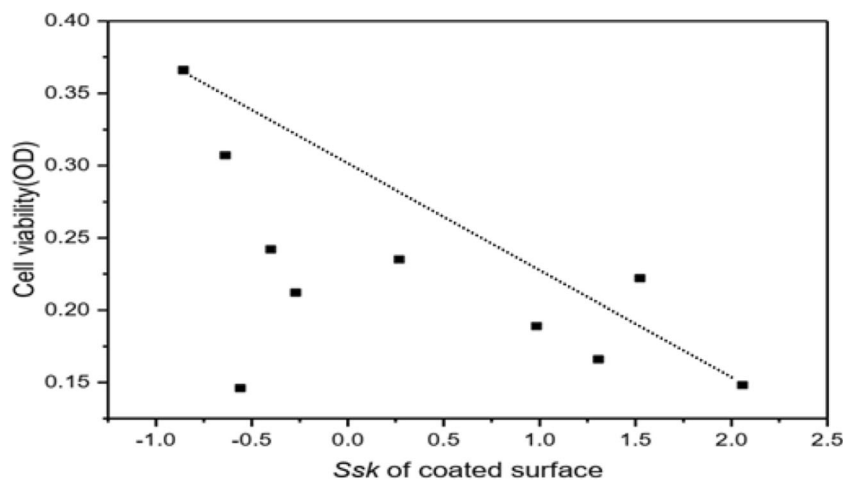**Fig. 10** Cell viability of implants

Figure 10 shows the cell viability chart for a different implant. The cells grown on the cell culture plate were the control sample implant which denoted 0.488 cell viability (OD). The thirteen sample implant plates are designated as a control sample, a to l. Nanoporous HA-$(Zn)_n$ coating structures with a pore size of 215–786 nm will assist cells attachment and its easy culture on the surface. There is an increase in surface area by 20 to 30% due to nanoporous structured surfaces; now, this excess area facilitates cells to adhere to the implant effortlessly. The implant (sample b) coated with 6 g/L HA concentration along with 1.6 g/L of zinc at 14 V power supply shows the highest cell viability with 0.366, and sample d showed least with 0.146. Furthermore, the increase in surface area exposes the infection to ZnO_2 which can prevent further infection of tissues, thereby increasing the life of the implant.

Effect of surface geometrical features on cell viability

Figure 11 shows the graph of cell viability (OD), which is plotted against the value of Ssk of the coated surfaces. It is found that negative Ssk values show higher cell viability
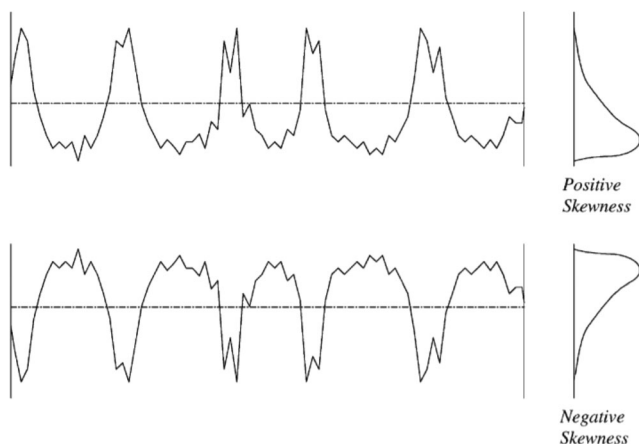
Fig. 12 Definition of skewness (*Ssk*) and amplitude distribution curve [24]

compared with the specimen with positive Ssk. The figure depicts that almost 60% of the coated samples show negative skewness values. It has been observed that for two different surfaces having almost the same range of surface roughness value shows different cell viability due to skewness of the surface. Based on the Table 2, implants samples b (Ssk = − 0.856), j (Ssk = 0.985) and g (Ssk = 1.524) have almost in the range of Sa (0.600–0.750 μm), but the cell viability for surface b is 64.86% higher than that of g (surface b: 0.366, surface g: 0.222). Moreover on comparing the cell viability of specimen g and j, the surface g shows 17.46% higher cell attachment. The surfaces with negative skewness depict broader peaks achieved during the coating process as shown in Fig. 12.

Previous studies have concluded that surface roughness alone is not a key factor in defining the scale of cell viability. Cell viability requires certain processes like protein adsorption and extension of filopodium which are dependent on surface characteristics like skewness (Ssk), kurtosis (Sku) and spatial distribution of peaks representing average height. Surfaces with negative skewness depict broader peaks, which facilitates huge exposure for cell adherence via cell-adhesive proteins by its filopodium. The surface topography with negative skewness value works as an important factor in improving cell adhesion; however, the value of Sku did not affect cell adhesion [25]. In the present study, the cell viability for implant specimen b is 64.86% higher than that of implant specimen g. It is because the cells preferentially adhered on the microstructure coated surfaces with the micropores array, which has lower Ssk (< 0) as compared with the surfaces which having sharp peaks (Ssk > 0).

Conclusions

The electrochemical deposition of HA and $(Zn)_n$ on the implant is performed, and SEM reveals that the nanoporous HA structures with a pore size of 215–786 nm are obtained which

is suitable for good biocompatibility. The coating thickness increases with increase in HAP, $(Zn)_n$ concentration and anodic voltage. Especially higher $(Zn)_n$ concentration and anodic voltage show the highest coating thickness of 14.76 μm. The study reveals that the cell viability is observed to be maximum at HA concentration of 6 g/L and $(Zn)_n$ concentration in the range of 0.8 to 1.2 g/L. The $(Zn)_n$ concentration in the range of 0.8 to 1.2 g/L and anodic voltage of 12–13 V is suitable for obtaining the controlled coating thickness. The least coating thickness of 4.30 μm is achieved during this process. The EDS mapping confirms the generation of oxide layers on the implant. The best parameters for cell viability are 6 g/L HA concentration, 1.6 g/L of $(Zn)_n$ and 14 V power supply showing the highest cell viability with 0.366 for 30-min coating time. Based on the surface geometrical features studies, the negative skewness value is found to be an important factor on cell viability. The HA-$(Zn)_n$ coatings developed would be preferably suitable for developing implant devices with enhanced osseointegration and improved lifetime for biomedical applications.

References

1. Geetha, M., Singh, A.K., Asokamani, R., Gogia, A.K.: Ti based biomaterials, the ultimate choice for orthopaedic implants–a review. Prog-Mater-Sci. **54**, 397–425 (2009)
2. Li, Y., Yang, C., Zhao, H., Qu, S., Li, X., Li, Y.: New developments of Ti-based alloys for biomedical applications. Materials. **7**, 1709–1800 (2014)
3. Vadakkumpurath, S., Venugopal, A.N., Llattil, S.: Influence of micro-textures on antibacterial behaviour of titanium-based implant surfaces: In vitro studies. Biosurf Biotribol. **5**, 20–23 (2019)
4. Niinomi, M., Nakai, M., Hieda, J.: Development of new metallic alloys for biomedical applications. Acta Biomater. **8**, 3888–3903 (2012)
5. Niinomi, M.: Mechanical properties of biomedical titanium alloys. Mater. Sci. Eng. C. **243**, 231–236 (1998)
6. Liu, X.B., Meng, X.J., Liu, H.Q., Shi, G.L., Wub, S.H., Sun, C.F., Wang, M.D., Qi, L.H.: Development and characterization of laser clad high temperature self-lubricating wear resistant composite coatings on Ti–6Al–4V alloy. Mater. Des. **55**, 404–409 (2014)
7. Minagar, S., Berndt, C.C., Wang, J., Ivanova, E., Wen, C.: A review of the application of anodization for the fabrication of nanotubes on metal implant surfaces. Acta Biomater. **8**, 2875–2888 (2012)
8. Hacioglu, T., Evis, Z., Tezcaner, A., Aydınol, M.K.: Effects of surface pretreatments and coating period on hydroxyapatite coating of Ti6Al4V alloy. J. Aust. Ceram. Soc. 1–13 (2019)
9. Søballe, K.: Hydroxyapatite ceramic coating for bone implant fixation: mechanical and histological studies in dogs. Acta Orthop. Scand. **64**, 1–58 (1993)
10. Daugaard, H., Elmengaard, B., Bechtold, J.E., Jensen, T., Soballe, K.: The effect on bone growth enhancement of implant coatings with hydroxyapatite and collagen deposited electrochemically and by plasma spray. J. Biomed. Mater. Res. A. **92**, 913–921 (2010)
11. Nuswantoro, N.F., Budiman, I., Septiawarman, A., Tjong, D.H., Manjas, M.: Effect of applied voltage and coating time on nano hydroxyapatite coating on titanium alloy Ti6Al4V using electrophoretic deposition for orthopaedic implant application. In: IOP Conference Series: Materials Science and Engineering, vol. 547, p. 012004. IOP Publishing (2019)
12. Rossi, L., Migliaccio, S., Corsi, A., Bianco, P., Teti, A., Gambelli, L., Cianfarani, S., Paoletti, F., Branca, F.: Reduced growth and skeletal changes in zinc-deficient growing rats are due to impaired growth plate activity and inanition. J. Nutr. **131**, 1142–1146 (2001)
13. Thanigaivelan, R., Arunachalam, R.M., Madhan, C., Kumar, R.R., Muthuselvam, M.: Impact of electrochemical passivation on Burr suppression of Ti–4Al–6V alloy during machining. Surf. Eng. Appl. Electrochem. **55**, 424–429 (2019)
14. Ur Rahman, Z., Pompa, L., Haider, W.: Influence of electropolishing and magnetoelectropolishing on corrosion and biocompatibility of titanium implants. J. Mater. Eng. **23**, 3907–3915 (2014)
15. Kar, A., Raja, K.S., Misra, M.: Electrodeposition of hydroxyapatite onto nanotubular TiO2 for implant applications. Surf. Coat. Technol. **201**, 3723–3731 (2006)
16. Manso, M., Jimenez, C., Morant, C., Herrero, P., Martínez-Duart, J.M.: Electrodeposition of hydroxyapatite coatings in basic conditions. Biomaterials. **21**, 755–1761 (2000)
17. Prasad, B.E., Kamath, P.V.: Electrodeposition of dicalcium phosphate dihydrate coatings on stainless steel substrates. Bull. Mater. Sci. **36**, 475–481 (2013)
18. Manonmani, R., Vinodhini, S.P., Venkatachalapathy, B., Sridhar, T.M.: Electrochemical, mechanical and osseointegration evaluation of NBPC-coated 316L SS by EPD. Surf. Eng. **34**, 511–519 (2018)
19. Qiu, D., Yang, L., Yin, Y., Wang, A.: Preparation and characterization of hydroxyapatite/titania composite coating on NiTi alloy by electrochemical deposition. Surf. Coat. Technol. **205**(10), 3280–3284 (2011)
20. Yan, Y., Zhang, X., Mao, H., Huang, Y., Ding, Q., Pang, X.: Hydroxyapatite/gelatin functionalized graphene oxide composite coatings deposited on TiO2 nanotube by electrochemical deposition for biomedical applications. Appl. Surf. Sci. **329**, 76–82 (2015)
21. Yang, F., Dong, W., He, F., Wang, X., Zhao, S., Yang, G.: Osteoblast response to porous titanium surfaces coated with zinc-substituted hydroxyapatite. Oral Surg. Oral Med. Oral Pathol. Oral Radiol. **113**, 313–318 (2012)
22. Takeda, I., Serizawa, S., Kaneko, A.: Fabrication of micro-structured scaffold using self-assembled particles and effects of surface geometries on cell adhesion. Mech Eng J. **3**, 1–8, 15–1–00521 (2016)
23. Thanigaivelan, R., Arunachalam, R.M., Nithish, A., Venkatesh, S., Naveenkumar, P., Selvaganapathy, S., Aravind, A.S.: Optimization of laser and electrochemical process parameters for surface modification of hardness and hydrophobicity on 316L steel. Laser Eng. **45**, 69–84 (2020)
24. Teng, H.P., Yang, C.J., Lin, J.F., Huang, Y.H., Lu, F.H.: A simple method to functionalize the surface of plasma electrolytic oxidation produced TiO$_2$ coatings for growing hydroxyapatite. Electrochim. Acta. **193**, 216–224 (2016)
25. Havlikova, J., Strasky, J., Vandrovcova, M., Harcuba, P., Mhaede, M., Janecek, M., Bacakova, L.: Innovative surface modification of Ti–6Al–4V alloy with a positive effect on osteoblast proliferation and fatigue performance. Mater. Sci. Eng. C. **39**, 371–379 (2014)